Published in final edited form as:
Dev Cell. 2013 November 11; 27(3): 319–330. doi:10.1016/j.devcel.2013.09.001.

Luminal mitosis drives epithelial cell dispersal within the branching ureteric bud

Adam Packard[1], **Kylie Georgas**[2], **Odyssé Michos**[1,#], **Paul Riccio**[1], **Cristina Cebrian**[1], **Alexander N. Combes**[2], **Adler Ju**[2], **Anna Ferrer-Vaquer**[4], **Anna-Katerina Hadjantonakis**[4], **Hui Zong**[3], **Melissa H. Little**[2], and **Frank Costantini**[1,*]

[1]Department of Genetics and Development, Columbia University, New York, NY 10032, USA

[2]Institute for Molecular Bioscience, The University of Queensland, St. Lucia, Brisbane 4072, Australia

[3]Dept of Microbiology, Immunology, and Cancer Biology, Center for Cell Signaling, Center for Brain Immunology and Glia, Neuroscience Graduate Program, University of Virginia School of Medicine, Charlottesville, VA 22908, USA

[4]Developmental Biology Program, Sloan-Kettering Institute, New York, NY 10065, USA

Summary

The ureteric bud is an epithelial tube that undergoes branching morphogenesis to form the renal collecting system. Though development of a normal kidney depends on proper ureteric bud morphogenesis, the cellular events underlying this process remain obscure. Here, we used time-lapse microscopy together with several genetic labeling methods to observe ureteric bud cell behaviors in developing mouse kidneys. We observed an unexpected cell behavior in the branching tips of the ureteric bud, which we term “mitosis-associated cell dispersal”. Pre-mitotic ureteric tip cells delaminate from the epithelium and divide within the lumen; while one daughter cell retains a basal process, allowing it to reinsert into the epithelium at the site of origin, the other daughter cell reinserts at a position one to three cell diameters away. Given the high rate of cell division in ureteric tips, this cellular behavior causes extensive epithelial cell rearrangements that may contribute to renal branching morphogenesis.

Introduction

The formation of branched epithelial ducts, a process known as branching morphogenesis, underlies the development of many organs (Affolter et al., 2009; Andrew and Ewald, 2010). In kidney development, the epithelial ureteric bud (UB) branches and elongates to give rise to the complex system of collecting ducts, which in the mature organ will convey urine from the distal tubules of the nephrons to the ureter and bladder (Bridgewater and Rosenblum, 2009; Costantini, 2012; Little et al., 2010; Nigam and Shah, 2009). The UB arises (at E10.5 in the mouse) as an outgrowth from the caudal region of the nephric duct, which is composed of pseudostratified epithelium (a type of epithelium in which the nuclei lie at different apical-basal levels, due to interkinetic nuclear migration) (Kosodo, 2012; Spear and

*Corresponding Author. fdc3@columbia.edu. 212-305-6814.
#Current Address: Sanger Institute, Wellcome Trust Genome Campus, Hinxton, Cambridgeshire, CB10 1HH, UK

Erickson, 2012). When the UB first branches within the metanephric mesenchyme at E11.5, it remains pseudostratified, but soon thereafter it converts to a single-layered epithelium (Chi et al., 2009b). Further growth and branching occurs by the expansion and continued re-shaping of this epithelial tree, which contains a lumen that is patent all the way to the tips (Meyer et al., 2004).

The cellular events that underlie branching morphogenesis, in kidney as well as other organs, remain poorly understood. Some of the cellular behaviors (among many others) that could potentially cause the UB epithelium to form new branches include localized cell proliferation, oriented cell division and cell movements (reviewed in Costantini, 2006). Cell proliferation is much higher in the terminal ampullae, or “tips”, of the UB (Fisher et al., 2001; Michael and Davies, 2004), where new branches form (Al-Awqati and Goldberg, 1998) (Watanabe and Costantini, 2004), compared to “trunks” (the tubular portions of the UB behind the tips, which are elongating, narrowing and beginning to differentiate). However, proliferation within the ampullae does not appear localized to the subdomains where new branches are emerging (Fisher et al., 2001; Michael and Davies, 2004). While oriented cell division has been implicated in the elongation of collecting ducts at later stages of kidney development (Fischer et al., 2006; Karner et al., 2009; Saburi et al., 2008; Yu et al., 2009), as well as in lung bud morphogenesis (Tang et al., 2011), it remains unclear if this mechanism plays a role in UB branching. Extensive cell movements have been shown to occur in the mouse nephric duct during formation of the initial UB, as well as during later UB branching, by time-lapse analysis of chimeric kidneys in which a subset of nephric duct or UB cells were labeled with GFP (Chi et al., 2009b; Shakya et al., 2005). However, the large number of labeled cells and the low resolution of imaging in these studies made it difficult to follow the behavior of individual UB cells and thus to discern their modes of movement.

For this reason, we used genetic strategies to label very small numbers of ureteric bud cells with fluorescent proteins, allowing us to follow their behavior by time-lapse microscopy in cultured kidneys. We also used kidneys from transgenic mice expressing membrane-associated, or nuclear, fluorescent proteins to follow UB cell behaviors at high resolution by 4-D confocal microscopy. These studies revealed an unexpected phenomenon, occurring in the terminal, branching regions of the UB epithelium. A pre-mitotic cell first delaminates from the epithelium into the lumen, retaining only a thin, membranous basal process. The cell then divides, one daughter inherits the basal process and reinserts into the epithelium at the site of origin, while the other daughter reinserts at a position 1–3 cell diameters away. We confirmed that cell divisions occur predominantly in the lumen of the branching UB, *in vivo*, by confocal microscopy of fixed kidneys at several stages of development. The mitosis-associated cell dispersal that we observe represents a mode of epithelial cell motility distinct from those that have been previously described. This mode of luminal division appears inconsistent with models in which epithelial growth is patterned by the orientation of cell divisions within the epithelium. Instead, it suggests that cell movements immediately following mitosis may contribute to branching morphogenesis in the kidney.

Results

Clonal analysis of ureteric bud tip cells reveals a type of cell motility coupled to mitosis

In attempts to study the behavior of ureteric bud cells during branching morphogenesis, we used several genetic methods to label small numbers of ureteric bud cells with a fluorescent protein. This allowed us to follow their division and movements, by time-lapse microscopy, in cultured kidney explants. The rare, labeled cells expressed a different fluorescent protein than the rest of the UB cells (e.g., red vs. green,), while the surrounding mesenchymal cells were unlabeled. Thus, we could clearly distinguish each labeled UB cell, and its daughters,

from the surrounding UB cells (details in Experimental Procedures and Figure 1 legend). In all cases, the differentially labeled cells were of the same genotype (except for fluorescent protein genes) as the surrounding cells.

E11.5 or E12.5 kidneys were explanted, cultured under standard conditions (Costantini et al., 2011), and photographed every 20–60 minutes with an inverted epifluorescence microscope, typically for 2–3 days. Labeled cells that were initially located at the lateral "edge" of a UB tip or terminal branch usually had a columnar appearance (Figure 1, "0 hr" panels). Many of these cells divided during culture (five examples of mitotic events are shown in Figure 1 and Movie S1 in Supplemental Material). Before division, the parental cell appeared to retract from the basal edge and move in an apical direction. This cell became large and round (e.g., Figure 1A, 2 hr; Figure 1B, 1.7 hr; Figure 1C, 5.7 hr; Figure 1D, 8 hr), and divided by the next frame (20 – 60 min later). Immediately after cytokinesis, while one daughter cell appeared to return to its initial position (indicated by asterisks in Figure 1A–D), the other daughter cell moved away, to a distance of approximately 1–3 cell diameters (e.g., Figure 1A, 2.5 hr; Figure 1B, 2 hr; Figure 1C, 6.3 hr; Figure 1D, 6 and 9 hr). The two daughter cells typically remained at this distance, or moved further apart, at subsequent times. Only very rarely (in 1 out of 21 mitotic events visualized by these methods) did the two daughter cells appear to remain immediately adjacent to each other (not shown). Thus, the mitosis of UB tip epithelial cells leads to the immediate relocation of one of the two daughter cells; we term this phenomenon "mitosis-associated cell dispersal". There was no discernible pattern of movement of the motile daughter cell; it moved towards the nearest extreme tip (e.g., Figure 1B, and Figure 1D upper tip) or away from the tip (e.g., Figure 1D lower tip), with similar frequencies.

4-D analysis with fluorescent membrane labels reveals that mitosis-associated cell dispersal occurs via transient delamination into the UB lumen

To follow the behavior of mitotic epithelial cells during UB branching morphogenesis with higher resolution, we cultured transgenic kidneys in which myrVenus, a membrane-associated fluorescent protein, is expressed in all ureteric bud cells (*Hoxb7/myrVenus*) (Chi et al., 2009a). In confocal optical sections, the outline of each UB cell is labeled by myrVenus, while the surrounding mesenchyme cells are unlabeled. We collected confocal image stacks through a branching UB tip, at 10-minute intervals over 21 hours (Figure 2A, B), and generated a 4D (3D time-lapse) movie. By examining different z-levels, we could focus either on the epithelia at the upper or lower surfaces of the UB (e.g., Figure 2B – first two and last two images) or on the central lumen (e.g., Figure 2A and central 2 panels of Figure 2B). A complete z-stack at one time point is shown in Movie S2). This indicated that the UB epithelium at E12.5 consisted mainly of a single layer of cells, but it also revealed that a few cells were transiently located in the luminal space (e.g., asterisks in Figure 2A, B).

Of 172 UB cell divisions we observed, only about 5% occurred within the confines of the epithelium (e.g., Figure 2C and Movie S3, first image sequence). Instead, in most cases (~95%), a cell about to divide first elongated into the UB lumen, then moved partially or fully into the luminal space, but retained contact with the adjacent epithelial cells (Figure 2D–F). These cells appear to correspond to the large, round mitotic cells seen in the lower-resolution time-lapse studies of Figure 1. The luminal location of these cells could also be seen in the z-dimension (Movie S2, and XZ-projection insets in Figure 2D–F). The cell then divided, after which one or both daughter cells could be seen to reinsert into the epithelium (Figure 2D–F, Movie S3). While not all the reinsertion events could be followed, there was no accumulation of cells in the UB lumen, suggesting that both daughter cells reinsert. The interval between the beginning of pre-mitotic cellular elongation and reinsertion was about 60–90 minutes.

Though these *Hoxb7/myrVenus*-labeled, mitotic UB cells did not appear to have a connection with the basal surface of the epithelium – because the fluorescence from neighboring cells obscured individual cell boundaries – it remained possible that these cells retained basal contact by way of a thin process. Thus, we needed to label a small subset of UB tip cells with a membrane-targeted fluorescent reporter and observe them as they completed delamination, mitosis, cytokinesis and reinsertion. For this purpose we used *mTmG* mice, in which every cell initially expresses the membrane-targeted red fluorescent protein "mT", but upon Cre-mediated recombination, permanently switches to express the membrane-targeted green fluorescent protein "mG" (Muzumdar et al., 2007). To induce recombinant clones in the terminal portions of the branching ureteric bud, we crossed *mTmG* mice with *Ret-CreERT2* transgenic mice (Luo et al., 2009), as the *Ret* gene is expressed specifically at the UB tips (Pachnis et al., 1993). E12.5 kidneys were treated in culture with a pulse of 4-OH tamoxifen, and confocal images stacks were collected at regular intervals.

Figure 3A shows an optical section through a branching UB ampulla, in which mT fluorescence allows the UB epithelium (circumscribed by a dotted line) to be distinguished from the surrounding mesenchyme, while an isolated mG-positive epithelial cell (white box) is about to undergo division, as shown in the optical sections of Figure 3B, B′ and 3D rendering in Figure 3B″. When the pre-mitotic UB cell translocates to the lumen (at 14′), it retains contact with the basal surface (dotted line) via a thin, membranous process (asterisk). During cytokinesis (28′), the basal process is inherited by one daughter cell (blue arrow) (see also Movie S4, which shows this dividing cell from different angles), which then reinserts into the epithelium at the position of the pre-mitotic basal process (42′, asterisk). The other daughter cell (yellow arrow), reenters the epithelium at a different position (56′ – 84′), while it is transiently connected to the stationary cell at its apical end (Figure S1 shows a second example of a cell division exhibiting the formation and asymmetric inheritance of a basal process). Among a total of 15 cell divisions observed in *mTmG* kidney cultures, in nine cases the luminal mitotic cell and its daughters displayed the behavior shown in Figures 3 and S1. We never observed a basal process being split and inherited by both daughter cells. Of the other six cases, five cells divided in the lumen, leading to daughter-cell dispersal, but formation of a basal process, or its inheritance, was not clearly visualized; the sixth cell divided within the epithelium (similar to the division shown in Figure 2C). Thus, the asymmetric inheritance of a basal process during most (if not all) luminal mitoses explains how one daughter cell reinserts into the epithelium at the starting position, while the other daughter is able to reinsert at a new site. Furthermore, the transient apical connection between the two daughter cells, which persists during at least the initial phase of reinsertion into the epithelium, probably limits the distance at which the motile daughter can reinsert.

Nuclear behaviors during mitosis-associated cell dispersal

To examine mitotic events at the nuclear level, we used *TcfLEF-H2BGFP* transgenic mice expressing a nuclear histone-GFP (Ferrer-Vaquer et al., 2010). This transgene is strongly expressed in ureteric bud cells of the developing kidney, at E12.5 (Burn et al., 2011; Ferrer-Vaquer et al., 2010) (Figure 4A–C), allowing us to follow nuclear dynamics during UB growth and branching in culture. E12.5 kidneys were cultured and confocal image stacks through the branching UB tips were collected at regular intervals (e.g., Figure 4B, C). A 4D rendering of this culture is shown in Movie S5. When the nuclei at individual z-levels were followed over time (Figure 4B, B′, C, C′ and Movie S6), very few cell divisions were visible at the level of the upper or lower epithelia (Figure 4B and C, and Movie S6). However, in optical sections bisecting the lumen, many mitotic figures were visible (Figure 4B′, C′, and Movie S6). Figure 4D, E and Movie S7 show examples of individual mitotic events. In these cases (as in most other mitoses), the nucleus moved in a luminal direction, divided, and the

daughter nuclei then moved back to the basal surface (pseudo-colored nuclei in Figure 4D, E). Only very rarely were mitotic events seen close to the basal surface (data not shown). While the apical surface of the epithelium (i.e., the edge of the lumen) was not visible using a nuclear marker, the movements of pre-mitotic nuclei in a luminal direction, and reinsertion of the daughter nuclei at two separate locations, are consistent with the cellular behaviors we observed using cytoplasmic or membrane markers (Figures 1–3, Movies S1 and S3–S4).

These time-lapse data also allowed us to analyze the locations of mitoses in the growing UB ampulla. The mitotic events were widely dispersed throughout the ampulla, and showed no evidence of clustering at the extreme tips, or in other locations (Figure S2). Thus, consistent with static analyses using BrdU incorporation (Fisher et al., 2001; Michael and Davies, 2004), our data argue against a role for localized cell proliferation in renal branching morphogenesis.

Many mitotic cells are found in the lumen of ureteric bud tips during kidney development *in vivo*

Our time-lapse studies of mitotic cell behaviors were conducted, by necessity, on kidneys developing in culture. To determine whether mitosis occurs in the UB lumen during kidney development *in vivo*, we analyzed kidneys in wholemount between E11.75, when branching has just begun, and E15.5, when branching is slowing and collecting duct elongation is beginning (Cebrian et al., 2004). The kidneys were imaged by confocal microscopy, following antibody staining against a panel of cellular markers; Calbindin1 (Calb1, UB epithelium), phosphohistone H3 (pHH3; mitotic cells), GFP (recognizing Six2-GFP in cap mesenchyme cells) and DAPI (all nuclei). Figure 5A shows one optical section through a ureteric tip at each of these stages (here, “tip” refers to the swollen terminal branches, and “trunk” to the deeper branches – see Figure 5G). pHH3+ UB cells were examined throughout the Z-stacks, and their locations were scored: within the lumen, at the border between lumen and epithelium, or within the epithelium (Figures 5B and S3). In the UB tips at E11.75 – E13.5, most mitotic cells (62–84%) were found within the lumen (Figure 5D). We confirmed that the luminal edge of the Calbindin1-positive epithelium corresponds to the apical surface (Figure S5). This supports our observations in organ cultures that most UB tip cells divide in the lumen. The luminal pHH3+ cells retained expression of Calbindin-1 and E-cadherin, suggesting they retain an epithelial phenotype (Figures 6 and S6), and projected beyond the apical surface defined by expression of apical marker ZO-1. Domains of ZO-1 expression were seen on some luminal cell membranes (Figure 6B). While this does not prove that apical-basal polarity is retained, the attachment of these cells to the basal lamina via a thin basal process suggests that this is the case.

At E14.5 and E15.5, the fraction of pHH3+ cells located within the tip lumen declined, while those at the luminal/epithelial border increased, and together these cells still accounted for more than half of the pHH3+ cells (Figure 5A, B, D). Occasional pHH3-negative, Calbindin1+, Ecad+ cells were also observed in the tip lumen (e.g. E12.5 in Figure 5A, Figure S6A, S6B and data not shown); these are likely to be post-mitotic cells that have not yet reinserted into the epithelium. To relate the locations of mitotic cells at different stages to other parameters of UB branching morphogenesis, we also counted pHH3+ cells per tip and measured luminal volume at E11.75 – E15.5. All of these parameters declined progressively after E12.5, with luminal volume dropping most dramatically (Figure 5C, Figure S4A–C).

Interestingly, cell division in the lumen appears to be a specific property of the branching tips of the ureteric bud epithelium. Unlike pHH3+ cells in the tips, pHH3+ cells in the trunks were most often located within the epithelium (Fig 5E, F, H), except at E12.5 when trunk lumens were large and around half of the mitosing cells were luminal (Figure 5G).

Despite the declining size of the tip lumen and percentage of luminal pHH3+ tip cells in fixed kidneys during later phases of development, time-lapse movies of the UB tips in cultured E17.5 kidneys revealed that many mitotic cells at this stage still undergo luminal translocation and dispersal of one daughter cell (Figure 7), as seen in earlier stage kidneys.

Discussion

Epithelial cells in many developing tissues are known to undergo extensive movements, resulting in changes in cell position and exchange of neighbors within the epithelium. The reported mechanisms of epithelial cell movement include lateral intercalation (Karner et al., 2009; Lecuit, 2005), rearrangement of rosettes (Lienkamp et al., 2012; Vichas and Zallen, 2011), and collective cell migration (Ewald et al., 2008; Vasilyev et al., 2009). Here, we describe a new and distinct type of cell movement, which is closely coupled to cell division in the branching regions of the ureteric bud; we term this process “mitosis-associated cell dispersal”. In time-lapse studies of cultured kidneys, we observed that nearly all pre-mitotic UB tip cells first elongate in the apical direction and then delaminate into the lumen before dividing. In most cases, the mitotic cell retains a very thin connection to the basal surface. The cell immediately divides, one daughter cell inheriting the basal process; this “tethered” daughter cell then reinserts into the epithelium at the position of origin, while the other (“motile”) daughter cell reinserts at a nearby, but non-contiguous, position. Consistent with these observations in live organ cultures, many mitotic (pHH3+) cells in fixed kidneys were found in the UB tip lumen. Given the high frequency of mitosis in the UB tips, this behavior results in frequent cell rearrangements, and is sufficient to explain the dispersion of clonally related cells observed in chimeric kidneys (Shakya et al., 2005). Mitosis-associated cell dispersal involves several kinds of cell movement: delamination of the pre-mitotic parental cell into the lumen, reinsertion of this cell back into the epithelium after mitosis, reinsertion of the other daughter cell at a new site, as well as the passive displacement of cells at the reinsertion site of the motile daughter.

The subcellular mechanisms of ureteric bud cell delamination, movement, and reinsertion remain to be elucidated. However, this process bears some similarities to the nuclear movements that occur in pseudostratified epithelia, known as interkinetic nuclear migration (IKNM) (Kosodo, 2012; Spear and Erickson, 2012). In pseudostratified epithelia, the nuclei oscillate between the apical and basal sides of the epithelium during the cell cycle, and cells divide mainly at the apical side, while retaining a thin connection to the basal surface. Unlike mitosis-associated cell dispersal in the UB, mitosis in pseudostratified epithelia occurs within the confines of the epithelium, and the daughter cells generally remain contiguous after cytokinesis (Das et al., 2003; Miyata et al., 2001). One interesting exception occurs in the developing neural keel of zebrafish embryos, where one daughter cell crosses the midline and reinserts in the neuroepithelium on the opposite side (Ciruna et al., 2006). Similar but less dramatic nuclear movements are commonly observed in columnar epithelia, where mitotic figures are generally observed at the apical side of, but within, the epithelium (e.g., Baker and Garrod, 1993; Raphael et al., 1994; Smart, 1970). In the branching UB epithelium, the nuclei of cells entering mitosis apparently initiate a similar apically-directed movement, but don’t stop at the apical surface of the epithelium, leading to cellular elongation and then delamination of the bulk of the cell into the lumen. The basal-to-apical movements that occur during IKNM in pseudostratified epithelia are mediated, in different systems, by either microtubules or the actin cytoskeleton (Kosodo, 2012; Spear and Erickson, 2012). Since the UB develops from the pseudostratified epithelium of the caudal nephric duct (Chi et al., 2009b), perhaps the apical movement of the nucleus, the initial step in mitosis-associated cell dispersal, is mechanistically related to the IKNM exhibited in the earlier pseudostratified epithelium. Recent work has provided increasing insight into the molecular mechanisms governing epithelial cell division in other systems (e.g., Bourdages

and Maddox, 2013; Guillot and Lecuit, 2013), and it will be important to determine the mechanistic differences that cause mitotic UB tip cells to delaminate from and reinsert into the epithelium. The UB tip epithelium is known to differ dramatically from trunk epithelium in patterns of gene expression (Caruana et al., 2006; Schmidt-Ott et al., 2005; Yu et al., 2012), but the differences in epithelial cell properties and interactions that allow mitosis-associated cell dispersal to occur specifically in the tips remain to be defined.

What might be the function of mitosis-associated cell dispersal? In the developing kidney, mitosis (and hence mitosis-associated cell dispersal) occurs predominantly in the tips, the terminal regions where new branches are forming. In the UB trunks, there is less frequent cell division, and luminal mitotic cells were observed, but only at E12.5, when the trunk lumens were large. Within ureteric trunk epithelium distant from the branching ampullae, after E12.5, as these tubules narrow, cell division occurs without mitosis-associated cell dispersal. Here, daughter cells remain contiguous (e.g., Figure 1 in Fischer et al, 2006). This suggests that mitosis-associated cell dispersal might be important to allow the very rapid cell division that occurs in UB tips. It has been observed that epithelia may act as a “suppressive environment” for cell division, and delamination into the lumen may allow a higher rate of cell division, albeit in a pathological context (Leung and Brugge, 2012). However, reinsertion into the epithelium was not observed in that study, nor would the ability of a UB cell to divide more readily in the lumen explain why one daughter cell reinserts at a different position. Alternatively, this cellular behavior might have a specific role in the reshaping of the UB tip epithelium that underlies branching morphogenesis. Since ~2% of UB tip cells are pHH3+ at any given time (Kuure et al., 2010), and assuming that the mitotic (pHH3-positive) phase lasts approximately one hour (Figures 2–4), then in each 24-hr period approximately half the cells in each UB tip will undergo mitosis-associated cell dispersal (and many others will be passively displaced), leading to extensive cell rearrangements. Even though the untethered daughter cells do not move far, if they tended to move in a non-random direction, the resulting directional “flow” of cells might cause the epithelium to expand in some regions more than others - reshaping the ampulla and thus contributing to branch formation. Further work is required to test this hypothesis.

Another possible (and related) role of mitosis-associated cell dispersal may be to influence cell fate. UB tip cells represent progenitor cells, some of whose daughter cells remain at the growing tip (i.e., in the progenitor pool), while other daughters are left behind in the trunk and begin to differentiate into collecting duct cells (Shakya et al., 2005) (P. R. and F.C., manuscript in preparation). It is not known how the daughters of individual dividing tip cells differ in their short-term fate (in the long term, all will become collecting duct cells), but it is likely that many divisions are asymmetric in that one daughter cell (and its progeny) will remain at the tip longer than the other. In terms of *cell position*, a luminal division in which one daughter reinserts at the same position, while the other daughter moves away, is inherently asymmetric. A further asymmetry is seen in the inheritance of the basal process, which appears to be retained by only one daughter UB cell. In the developing nervous system, progenitor cells divide at the apical side of (but within) the neuroepithelium, and a similar basal process connects the apical mitotic cell to the basal lamina; the basal process is usually inherited by only one daughter cell, and in asymmetric, neurogenic divisions, inheritance of the basal process may be an important determinant of cell fate (Fietz and Huttner, 2011; Kosodo and Huttner, 2009). This suggests that asymmetric inheritance of the basal process may also influence UB tip cell fate. It is also important to establish how the apical membrane is divided between daughter UB cells, as apical components can influence cell fate in many situations (Knoblich, 2008). It remains unclear whether the tethered and motile daughter UB cells have different fates and, if so, whether mitosis-associated cell movements or the inheritance of basal or apical components affect these fates. Answering these questions may require observing a mitotic event, including the inheritance of basal and

apical components by the tethered and motile daughter cell, and then following the fates of these daughter cells during an extended period of growth in organ culture.

An important implication of this finding concerns the potential role of oriented cell division (OCD) in ureteric bud branching. When cells divide within, and parallel to, an epithelium, the separation of the two daughter cells can exert directional forces on neighboring cells, leading to anisotropic tissue growth (Strutt, 2005). OCD is believed to contribute to the elongation of the collecting ducts in late fetal and adult mouse kidneys (Fischer et al., 2006; Karner et al., 2009; Saburi et al., 2008; Yu et al., 2009), and to the patterned growth of several other developing epithelia (Baena-Lopez et al., 2005; Sausedo et al., 1997; Tuckett and Morriss-Kay, 1985). However, when cells delaminate from the epithelium, divide in the lumen, and then reinsert into the epithelium at different positions, it seems very unlikely that the mitotic orientation could have such an effect. This conclusion is consistent with the observation that mitotic orientation was essentially random in kidneys tubules at E13.5 and E15.5 (Karner et al., 2009) (although the branching UB tip regions were not specifically examined in that study). Thus, cellular mechanisms other than OCD are likely to determine the patterns of epithelial morphogenesis during renal branching.

Mitosis-associated cell dispersal is apparently not a universal property of all rapidly growing epithelia. In many developing epithelia (e.g., fly wing disc), clonally related cells tend to remain closely associated, rather than immediately dispersing (Baena-Lopez et al., 2005; Fischer et al., 2006; Knox and Brown, 2002). What about branching epithelia besides kidney? While lineage tracing studies in developing lung epithelium indicate that clonal cells move apart (Rawlins et al., 2009), it was not determined if this cell dispersal occurred at the time of mitosis, as we observe in the UB, or later and by another mechanism. Our analysis of pHH3+ cells in fixed fetal lungs at E12.5 or E13.5 indicated that all pHH3+ nuclei were contained within the confines of the epithelium (data not shown). This would be consistent with evidence that OCD plays an important role in the patterns of lung bud morphogenesis (Tang et al., 2011); however, time-lapse live imaging of mitotic cell behaviors in lung and other branching epithelia will be required to determine if mitosis-associated cell dispersal is unique to kidney or is a more general phenomenon.

Experimental Procedures

Mouse strains and embryo staging

The sparsely labelled UB cells in Figure 1 were induced using several transgenic strains. The kidney in Figure 1A carried *Hoxb7/myrVenus* (*Tg(Hoxb7-Venus*)17Cos*), thus expressing a membrane-associated form green fluorescent protein in every UB cell (Chi et al., 2009a), the UB tip-specific inducible *Ret-CreERT2* allele (*Rettm2(cre/ERT2)Ddg*) (Luo et al., 2009), and the Cre-reporter line *Gt(ROSA)26Sortm1.1Hjf,* which expresses tdRFP1 after recombination (Luche et al., 2007). The kidney was explanted at E11.5, cultured for 1 hr with 100 nM 4OH-tamoxifen, rinsed and cultured in normal medium. The kidneys in Figure 1B and 1C express a low level of GFP throughout the UB, from the transgene *Hoxb7/CreGFP* (*Tg(Hoxb7-cre)5526Cmb*) (Zhao et al., 2004). The rare yellow cells express a higher level of GFP together with tdTomato, resulting in a yellow cell on the green UB background. Expression of the GFP and tdTomato was induced by a rare interchromosomal recombination event, catalysed by the CreGFP, between the *Gt(ROSA)26Sortm6(ACTB-EGFP*,-tdTomato)Luo/J* and *Gt(ROSA)26Sortm7(ACTB-EGFP*)Luo/J* loci on the two homologs of chromosome 6, as described (Tasic et al., 2012). The kidney in Figure 1D carries *Hoxb7/Cre* (*Tg(Hoxb7-cre)13Amc*) (Yu et al., 2002) and expresses cyan fluorescent protein throughout the UB (weakly visible in the GFP channel), due to recombination of the *Rosa26R-CFP* allele (*Gt(ROSA)26Sortm2(ECFP)Cos*) (Srinivas et al., 2001) catalyzed by Cre. The rare yellow cells are labeled in a similar manner to those in Figure 1B, C, but by

interchromosomal recombination between the *Tg(ACTB-EGFP,-tdTomato)11Luo/J* and *Tg(ACTB-tdTomato,-EGFP)11Luo/J* loci on chromosome 11 (Hippenmeyer et al., 2010).

The kidney in Figure 2 carries the *Hoxb7/myrVenus* transgene. The kidneys in Figure 3 and Figure S1 carry the *Rosa26-mTmG* Cre reporter allele (*Gt(ROSA)26Sortm4(ACTB-tdTomato,-EGFP)Luo/J*) (Muzumdar et al., 2007) and the *Ret-CreERT2* allele. The kidney was excised at E12.5, cultured, and recombination was induced in a small subset of UB tip cells (resulting in deletion of the gene encoding membrane-tethered tdTomato, "mT", and expression of membrane-tethered EGFP, or "mG") by treatment with 50nM 4-OH tamoxifen at 37°C for one hour. Kidneys were cultured for 24 hours to allow detectible levels of mG to accumulate in recombined cells before imaging. 3D rendering was performed using NIS Elements software with Golay filter deconvolution. The kidneys in Figure 4 and Figure S2 carry the transgene *TCF/Lef-H2BGFP* (*Tg(TCF/Lef1-HIST1H2BB/EGFP)61Hadj*) (Ferrer-Vaquer et al., 2010). The green cells in panels 4D and 4E were pseudo-colored using Adobe Photoshop. The kidney in Figure 7 carries both *Hoxb7/myrVenus* and *TCF/Lef-H2BGFP*. While *TCF/Lef-H2BGFP* is expressed in most or all UB cells at earlier stages, at E17 expression is limited to a subset of UB cells. mVenus and GFP signals were separated into distinct channels during imaging, using spectral detection and linear unmixing.

For wholemount kidney immunofluorescence, embryos were collected from timed matings of C57BL6 (for ZO-1 and aPKC wholemount data) or *Six2TGC* mice (*Tg(Six2-EGFP/cre)1Amc/J*) Kobayashi et al., 2008; (for all other wholemount data). In all experiments, noon of the day on which the mating plug was observed designated 0.5 embryonic days (E0.5).

All experiments with animals were performed with the approval of the Institutional Animal Care and Use Committees.

Kidney cultures and time-lapse imaging

Kidneys were cultured on Transwell-Clear filters in glass-bottom petri dishes, in environmentally controlled chambers, as previously described (Costantini et al., 2011). Time-lapse imaging was performed using Nikon TE300 or Zeiss Axio Observer Z1 epifluorescence microscopes (Figure 1), a Leica SP5 confocal microscope (Figure 2), and a Nikon A1R MP confocal microscope (Figures 3, 4, 7, S1 and S2).

Antibodies

Primary antibodies used for wholemount kidney immunofluorescence were: mouse anti-Calbindin1 (Calbindin D28K, Sigma C9848), rabbit anti-phospho-Histone H3 (pHH3, Ser10, Cell Signaling Technology 06-570) or rat anti-phospho-Histone H3 (pHH3, pSer28, Sigma-Aldrich H9908), chicken anti-GFP (Abcam ab13970) to detect Six2-EGFP, mouse anti-E-cadherin (BD Biosciences 610181), rabbit anti-ZO-1 (Life Technologies 40-2300), rabbit anti-PKC zeta (aPKC, Santa Cruz sc-216). Alexa fluor-conjugated secondary antibodies (Life Technologies) were used to detect primary antibodies and DAPI (Sigma Aldrich #D8417) was used to label nuclei.

Wholemount kidney immunofluorescence and confocal microscopy

Kidneys were isolated in phosphate buffered saline (PBS) and fixed with 4% paraformaldehyde in PBS for 10 min. They were then rinsed twice with PBS and transferred into PBS 0.1% triton-X 100 (PBTX), blocked in PBTX with 10% heat inactivated sheep serum for >1 h before being incubated for 12–48 h at 4 °C with primary antibody. After thoroughly washing with PBTX (8–24 h), the kidneys were incubated for 12–30 h at 4 °C with secondary antibody. Samples were then incubated with DAPI at 1:2000 for >1.5 hours

before being dehydrated with methanol (MeOH) in PBTX, 10 min at each stage: 25% MeOH in PBTX, 50%, 75%, 100%, 100%. After the final MeOH wash, samples were transferred into a glass bottom imaging dish (Mattek P35G-1.5-14-C) using a wide bore plastic transfer pipette. The remaining alcohol was removed from the dish with a P1000 pipette then a small amount of 1:2 Benzyl Alcohol (Sigma Aldrich 402834-1L) to Benzyl Benzoate (Sigma Aldrich B6630-1L)- BABB, was added to clear the samples. Samples were then imaged on an inverted Zeiss LSM 510 Meta confocal microscope.

Wholemount kidney image analysis

Z stacks (1.9μm intervals over 70–145μm) were obtained from the surface of immunofluorescently labeled wholemount kidneys (3–4 kidneys from each stage). Subsequently, image stacks were visualized using LSM image browser to score the location of pHH3+ nuclei as shown in Figure S2. Ureteric tips were distinguished from trunks using 3D structural morphology and by the presence of an adjacent Six2-labeled cap mesenchyme (Fig 5F–H). To obtain ureteric tip lumen volume and count pHH3+ cells, Z stacks were visualized in Imaris (Version 7.2, Bitplane AG). Ureteric tip lumen and epithelium surfaces were rendered using the edge of the Calbindin1 signal and Imaris Isolines function, while pHH3+ cell numbers were counted using Imaris spot count function as shown in Figure S4A. Ureteric tips were separated from ureteric trunks by manually cutting the tips from the Calbindin1 rendered 3D surface of the tree, perpendicular to where the tip joined the trunk. The number of pHH3+ cells in tips vs. trunks (Figure 5E) was compared using a Fisher's exact test of independence.

Supplementary Material

Refer to Web version on PubMed Central for supplementary material.

Acknowledgments

We thank Adam B. White and Theresa Swayne for help with confocal microscopy, James Lefevre for help with statistical analysis, and Carl Bates, Hideki Enomoto, Joerg Fehling, Liqun Luo, and Andrew McMahon for kindly providing mouse strains. ML is an NHMRC Senior Principal Research Fellow. This work was supported by grants from the NIH to FC (5R01DK083289) and AP (1F32DK096782) and from the NHMRC to ML (APP1002748).

References

Affolter M, Zeller R, Caussinus E. Tissue remodelling through branching morphogenesis. Nat Rev Mol Cell Biol. 2009; 10:831–842. [PubMed: 19888266]

Al-Awqati Q, Goldberg MR. Architectural patterns in branching morphogenesis in the kidney. Kidney International. 1998; 54:1832–1842. [PubMed: 9853247]

Andrew DJ, Ewald AJ. Morphogenesis of epithelial tubes: Insights into tube formation, elongation, and elaboration. Dev Biol. 2010; 341:34–55. [PubMed: 19778532]

Baena-Lopez LA, Baonza A, Garcia-Bellido A. The orientation of cell divisions determines the shape of Drosophila organs. Curr Biol. 2005; 15:1640–1644. [PubMed: 16169485]

Baker J, Garrod D. Epithelial cells retain junctions during mitosis. J Cell Sci. 1993; 104(Pt 2):415–425. [PubMed: 7685036]

Bourdages KG, Maddox AS. Dividing in epithelia: cells let loose during cytokinesis. Dev Cell. 2013; 24:336–338. [PubMed: 23449467]

Bridgewater D, Rosenblum ND. Stimulatory and inhibitory signaling molecules that regulate renal branching morphogenesis. Pediatr Nephrol. 2009; 24:1611–1619. [PubMed: 19083023]

Burn SF, Webb A, Berry RL, Davies JA, Ferrer-Vaquer A, Hadjantonakis AK, Hastie ND, Hohenstein P. Calcium/NFAT signalling promotes early nephrogenesis. Dev Biol. 2011; 352:288–298. [PubMed: 21295565]

Caruana G, Cullen-McEwen L, Nelson AL, Kostoulias X, Woods K, Gardiner B, Davis MJ, Taylor DF, Teasdale RD, Grimmond SM, et al. Spatial gene expression in the T-stage mouse metanephros. Gene Expr Patterns. 2006; 6:807–825. [PubMed: 16545622]

Cebrian C, Borodo K, Charles N, Herzlinger DA. Morphometric index of the developing murine kidney. Dev Dyn. 2004; 231:601–608. [PubMed: 15376282]

Chi X, Hadjantonakis AK, Wu Z, Hyink D, Costantini F. A transgenic mouse that reveals cell shape and arrangement during ureteric bud branching. Genesis. 2009a; 47:61–66. [PubMed: 19111008]

Chi X, Michos O, Shakya R, Riccio P, Enomoto H, Licht JD, Asai N, Takahashi M, Ohgami N, Kato M, et al. Ret-dependent cell rearrangements in the Wolffian duct epithelium initiate ureteric bud morphogenesis. Dev Cell. 2009b; 17:199–209. [PubMed: 19686681]

Ciruna B, Jenny A, Lee D, Mlodzik M, Schier AF. Planar cell polarity signalling couples cell division and morphogenesis during neurulation. Nature. 2006; 439:220–224. [PubMed: 16407953]

Costantini F. Renal branching morphogenesis: concepts, questions, and recent advances. Differentiation. 2006; 74:402–421. [PubMed: 16916378]

Costantini F. Genetic controls and cellular behaviors in branching morphogenesis of the renal collecting system. Wiley Interdiscip Rev Dev Biol. 2012; 1:693–713. [PubMed: 22942910]

Costantini F, Watanabe T, Lu B, Chi X, Srinivas S. Dissection of embryonic mouse kidney, culture in vitro, and imaging of the developing organ. Cold Spring Harb Protoc. 2011; 2011

Das T, Payer B, Cayouette M, Harris WA. In vivo time-lapse imaging of cell divisions during neurogenesis in the developing zebrafish retina. Neuron. 2003; 37:597–609. [PubMed: 12597858]

Ewald AJ, Brenot A, Duong M, Chan BS, Werb Z. Collective epithelial migration and cell rearrangements drive mammary branching morphogenesis. Dev Cell. 2008; 14:570–581. [PubMed: 18410732]

Ferrer-Vaquer A, Piliszek A, Tian G, Aho RJ, Dufort D, Hadjantonakis AK. A sensitive and bright single-cell resolution live imaging reporter of Wnt/ss-catenin signaling in the mouse. BMC Dev Biol. 2010; 10:121. [PubMed: 21176145]

Fietz SA, Huttner WB. Cortical progenitor expansion, self-renewal and neurogenesis-a polarized perspective. Curr Opin Neurobiol. 2011; 21:23–35. [PubMed: 21036598]

Fischer E, Legue E, Doyen A, Nato F, Nicolas JF, Torres V, Yaniv M, Pontoglio M. Defective planar cell polarity in polycystic kidney disease. Nat Genet. 2006; 38:21–23. [PubMed: 16341222]

Fisher CE, Michael L, Barnett MW, Davies JA. Erk MAP kinase regulates branching morphogenesis in the developing mouse kidney. Development. 2001; 128:4329–4338. [PubMed: 11684667]

Guillot C, Lecuit T. Mechanics of epithelial tissue homeostasis and morphogenesis. Science. 2013; 340:1185–1189. [PubMed: 23744939]

Hippenmeyer S, Youn YH, Moon HM, Miyamichi K, Zong H, Wynshaw-Boris A, Luo L. Genetic mosaic dissection of Lis1 and Ndel1 in neuronal migration. Neuron. 2010; 68:695–709. [PubMed: 21092859]

Karner CM, Chirumamilla R, Aoki S, Igarashi P, Wallingford JB, Carroll TJ. Wnt9b signaling regulates planar cell polarity and kidney tubule morphogenesis. Nat Genet. 2009; 41:793–799. [PubMed: 19543268]

Knoblich JA. Mechanisms of asymmetric stem cell division. Cell. 2008; 132:583–597. [PubMed: 18295577]

Knox AL, Brown NH. Rap1 GTPase regulation of adherens junction positioning and cell adhesion. Science. 2002; 295:1285–1288. [PubMed: 11847339]

Kosodo Y. Interkinetic nuclear migration: beyond a hallmark of neurogenesis. Cell Mol Life Sci. 2012; 69:2727–2738. [PubMed: 22415322]

Kosodo Y, Huttner WB. Basal process and cell divisions of neural progenitors in the developing brain. Dev Growth Differ. 2009; 51:251–261. [PubMed: 19379277]

Kuure S, Chi X, Lu B, Costantini F. The transcription factors Etv4 and Etv5 mediate formation of the ureteric bud tip domain during kidney development. Development. 2010; 137:1975–1979. [PubMed: 20463033]

Lecuit T. Adhesion remodeling underlying tissue morphogenesis. Trends Cell Biol. 2005; 15:34–42. [PubMed: 15653076]

Leung CT, Brugge JS. Outgrowth of single oncogene-expressing cells from suppressive epithelial environments. Nature. 2012; 482:410–413. [PubMed: 22318515]

Lienkamp SS, Liu K, Karner CM, Carroll TJ, Ronneberger O, Wallingford JB, Walz G. Vertebrate kidney tubules elongate using a planar cell polarity-dependent, rosette-based mechanism of convergent extension. Nat Genet. 2012; 44:1382–1387. [PubMed: 23143599]

Little M, Georgas K, Pennisi D, Wilkinson L. Kidney development: two tales of tubulogenesis. Curr Top Dev Biol. 2010; 90:193–229. [PubMed: 20691850]

Luche H, Weber O, Nageswara Rao T, Blum C, Fehling HJ. Faithful activation of an extra-bright red fluorescent protein in “knock-in” Cre-reporter mice ideally suited for lineage tracing studies. Eur J Immunol. 2007; 37:43–53. [PubMed: 17171761]

Luo W, Enomoto H, Rice FL, Milbrandt J, Ginty DD. Molecular identification of rapidly adapting mechanoreceptors and their developmental dependence on ret signaling. Neuron. 2009; 64:841–856. [PubMed: 20064391]

Meyer TN, Schwesinger C, Bush KT, Stuart RO, Rose DW, Shah MM, Vaughn DA, Steer DL, Nigam SK. Spatiotemporal regulation of morphogenetic molecules during in vitro branching of the isolated ureteric bud: toward a model of branching through budding in the developing kidney. Dev Biol. 2004; 275:44–67. [PubMed: 15464572]

Michael L, Davies JA. Pattern and regulation of cell proliferation during murine ureteric bud development. J Anat. 2004; 204:241–255. [PubMed: 15061751]

Miyata T, Kawaguchi A, Okano H, Ogawa M. Asymmetric inheritance of radial glial fibers by cortical neurons. Neuron. 2001; 31:727–741. [PubMed: 11567613]

Muzumdar MD, Tasic B, Miyamichi K, Li L, Luo L. A global double-fluorescent Cre reporter mouse. Genesis. 2007; 45:593–605. [PubMed: 17868096]

Nigam SK, Shah MM. How does the ureteric bud branch? J Am Soc Nephrol. 2009; 20:1465–1469. [PubMed: 19056872]

Pachnis V, Mankoo BS, Costantini F. Expression of the *c-ret* proto-oncogene during mouse embryogenesis. Development. 1993; 119:1005–1017. [PubMed: 8306871]

Raphael Y, Adler HJ, Wang Y, Finger PA. Cell cycle of transdifferentiating supporting cells in the basilar papilla. Hear Res. 1994; 80:53–63. [PubMed: 7852203]

Rawlins EL, Clark CP, Xue Y, Hogan BL. The Id2+ distal tip lung epithelium contains individual multipotent embryonic progenitor cells. Development. 2009; 136:3741–3745. [PubMed: 19855016]

Saburi S, Hester I, Fischer E, Pontoglio M, Eremina V, Gessler M, Quaggin SE, Harrison R, Mount R, McNeill H. Loss of Fat4 disrupts PCP signaling and oriented cell division and leads to cystic kidney disease. Nat Genet. 2008; 40:1010–1015. [PubMed: 18604206]

Sausedo RA, Smith JL, Schoenwolf GC. Role of nonrandomly oriented cell division in shaping and bending of the neural plate. J Comp Neurol. 1997; 381:473–488. [PubMed: 9136804]

Schmidt-Ott KM, Yang J, Chen X, Wang H, Paragas N, Mori K, Li JY, Lu B, Costantini F, Schiffer M, et al. Novel regulators of kidney development from the tips of the ureteric bud. J Am Soc Nephrol. 2005; 16:1993–2002. [PubMed: 15917337]

Shakya R, Watanabe T, Costantini F. The role of GDNF/Ret signaling in ureteric bud cell fate and branching morphogenesis. Dev Cell. 2005; 8:65–74. [PubMed: 15621530]

Smart IH. Changes in location and orientation of mitotic figures in mouse oesophageal epithelium during the development of stratification. J Anat. 1970; 106:15–21. [PubMed: 5413563]

Spear PC, Erickson CA. Interkinetic nuclear migration: a mysterious process in search of a function. Dev Growth Differ. 2012; 54:306–316. [PubMed: 22524603]

Srinivas S, Watanabe T, Lin CS, William CM, Tanabe Y, Jessell TM, Costantini F. Cre reporter strains produced by targeted insertion of EYFP and ECFP into the ROSA26 locus. BMC Dev Biol. 2001; 1:4. [PubMed: 11299042]

Strutt D. Organ shape: controlling oriented cell division. Curr Biol. 2005; 15:R758–759. [PubMed: 16169474]

Tang N, Marshall WF, McMahon M, Metzger RJ, Martin GR. Control of mitotic spindle angle by the RAS-regulated ERK1/2 pathway determines lung tube shape. Science. 2011; 333:342–345. [PubMed: 21764747]

Tasic B, Miyamichi K, Hippenmeyer S, Dani VS, Zeng H, Joo W, Zong H, Chen-Tsai Y, Luo L. Extensions of MADM (mosaic analysis with double markers) in mice. PLoS One. 2012; 7:e33332. [PubMed: 22479386]

Tuckett F, Morriss-Kay GM. The kinetic behaviour of the cranial neural epithelium during neurulation in the rat. J Embryol Exp Morphol. 1985; 85:111–119. [PubMed: 3989446]

Vasilyev A, Liu Y, Mudumana S, Mangos S, Lam PY, Majumdar A, Zhao J, Poon KL, Kondrychyn I, Korzh V, et al. Collective cell migration drives morphogenesis of the kidney nephron. PLoS Biol. 2009; 7:e9. [PubMed: 19127979]

Vichas A, Zallen JA. Translating cell polarity into tissue elongation. Semin Cell Dev Biol. 2011; 22:858–864. [PubMed: 21983030]

Watanabe T, Costantini F. Real-time analysis of ureteric bud branching morphogenesis in vitro. Dev Biol. 2004; 271:98–108. [PubMed: 15196953]

Yu J, Carroll TJ, McMahon AP. Sonic hedgehog regulates proliferation and differentiation of mesenchymal cells in the mouse metanephric kidney. Development. 2002; 129:5301–5312. [PubMed: 12399320]

Yu J, Carroll TJ, Rajagopal J, Kobayashi A, Ren Q, McMahon AP. A Wnt7b-dependent pathway regulates the orientation of epithelial cell division and establishes the cortico-medullary axis of the mammalian kidney. Development. 2009; 136:161–171. [PubMed: 19060336]

Yu J, Valerius MT, Duah M, Staser K, Hansard JK, Guo JJ, McMahon J, Vaughan J, Faria D, Georgas K, et al. Identification of molecular compartments and genetic circuitry in the developing mammalian kidney. Development. 2012; 139:1863–1873. [PubMed: 22510988]

Zhao H, Kegg H, Grady S, Truong HT, Robinson ML, Baum M, Bates CM. Role of fibroblast growth factor receptors 1 and 2 in the ureteric bud. Dev Biol. 2004; 276:403–415. [PubMed: 15581874]

Highlights

- Most pre-mitotic ureteric bud tip cells delaminate into the lumen before dividing.
- One daughter cell inherits a thin basal process and reinserts at the original site.
- The other daughter cell reinserts into the epithelium at a noncontiguous site.
- This form of cell movement results in extensive epithelial cell rearrangements.

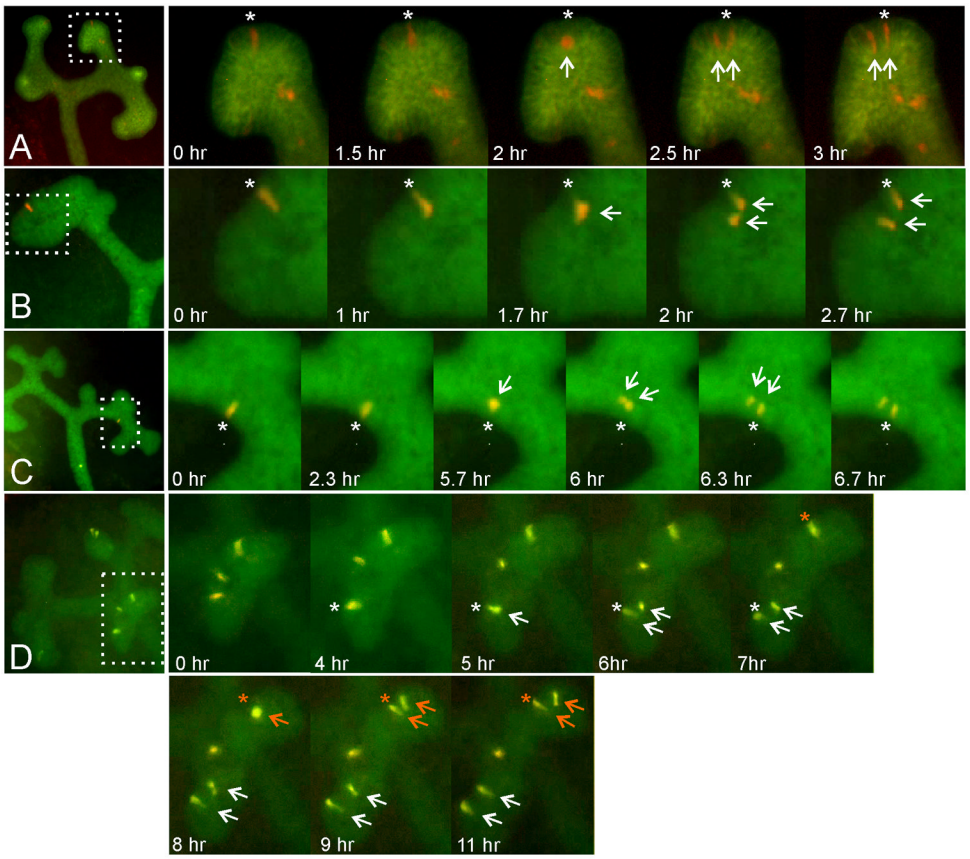

Figure 1. Time-lapse clonal analysis of labeled ureteric bud cells undergoing mitosis in cultured kidneys

Rare, differentially labeled ureteric bud cells were generated in mouse kidneys by several methods (see Experimental Procedures for details) and followed by time-lapse fluorescence microscopy of organ cultures. Five mitotic events are shown (one each in series **A–C**, two in series **D**). The four panels at left show low-magnification views of the kidneys before mitosis of the labeled cell(s). The panels on the right are enlargements, showing the starting position of the pre-mitotic cell (asterisk), movement of the cell away from the basal edge (arrow), cell division and immediate separation of the daughter cells (two arrows), reinsertion of one daughter cell at the site of origin (asterisk) and of the other cell at a distance. In **A**, the entire ureteric bud expresses the green fluorescent protein myrVenus, while a few cells express the red fluorescent protein tdRFP1. In **B** and **C**, the entire ureteric bud expresses eGFP, while a single cell expresses the red fluorescent protein tdTomato. In **D**, the entire ureteric bud expresses cyan fluorescent protein (weakly visible in the green channel), while a few cells co-express tdTomato and GFP. The image sequences in A–D are also shown in Movie S1.

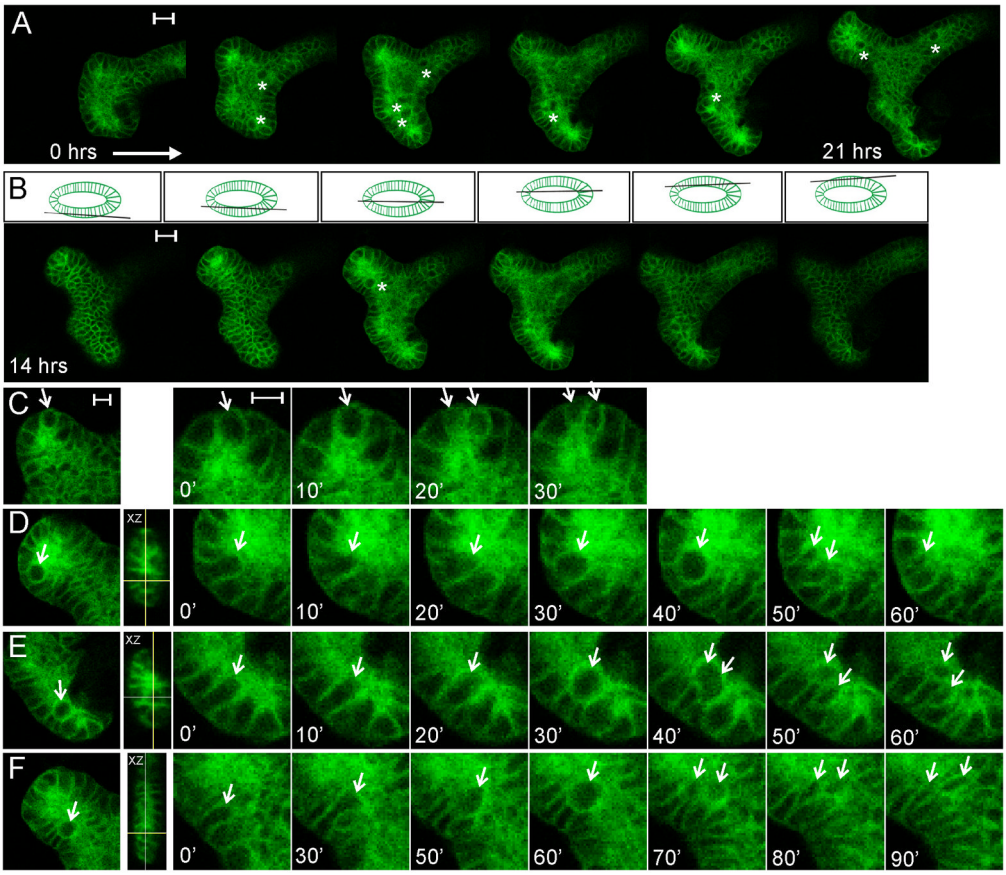

Figure 2. 4D confocal microscopic analysis of UB mitotic cell behaviors in a kidney culture, using the membrane-targeted fluorescent marker Hoxb7/myrVenus

A, optical sections through the center of a branching ureteric bud ampulla (bisecting the lumen), at six time points between the start (approximately E12.5) and end of the kidney culture (21 hours later). Asterisks indicate large, round mitotic cells visible within the lumen. **B**, at each time point a complete z-stack (1 μm spacing) was collected. Selected optical sections (at t=14hrs) are shown, starting at the outside of the lower epithelium, going through the center, and ending at the top of the upper epithelium (as indicated by the diagram above each image). For the complete z-stack, see Movie S2. **C**, a mitotic event in which the dividing cell remains within the epithelium. The image at left shows a UB tip with a large cell, apparently at metaphase; the next four images show enlargements of the dividing cell at 10 minute intervals. **D–F**, three examples of cell divisions within the UB lumen. The left image in each case shows the location of the mitotic cell at lower magnification. The next image is an XZ projection showing the location of the mitotic cell (crosshairs) within the lumen. The images at right show the sequence of: elongation of the pre-mitotic cell towards the lumen; delamination into the lumen and enlargement of the mitotic cell; cytokinesis; and reinsertion of one daughter cell at the original position in the surface epithelium. In E and F, the second daughter cell has not reinserted at the same position; in D, the second daughter cell is not seen (presumably after reinsertion at a different z-level). (The sequences in C–F are also shown in Movie S3). Scale bars 20 μm (A, B) or 10 μm (C; same for D–F).

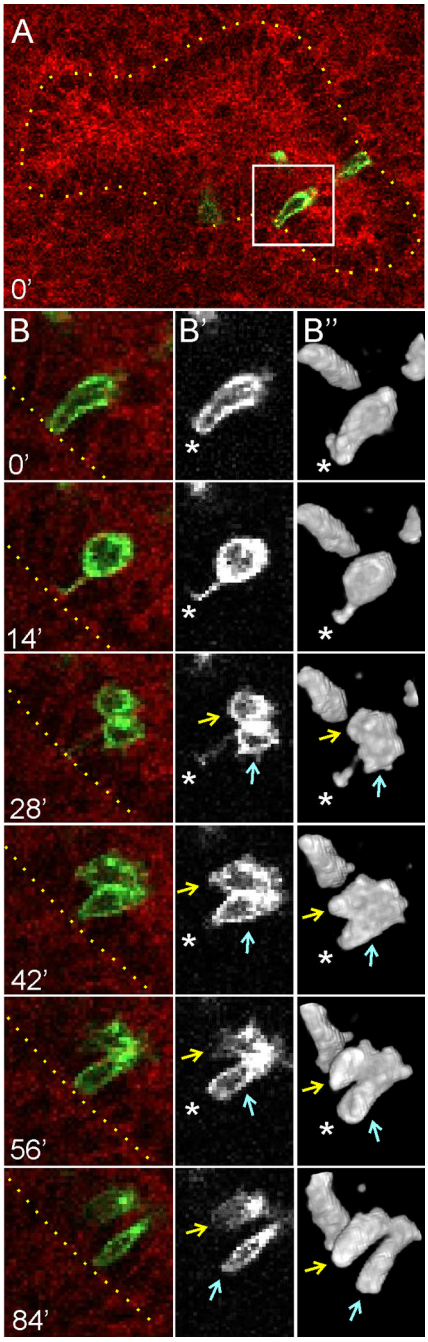

Figure 3. 4D confocal microscopic analysis of a dividing UB cell in a kidney culture, using dual-colored, membrane-targeted fluorescent markers

A, optical section through a branching ureteric bud ampulla (at a z-level bisecting the lumen) in a *mTmG*/+, *Ret-CreERT2*/+ kidney. The kidney was explanted at E12.5, treated with 4-OH tamoxifen, and cultured overnight before confocal images stacks (0.75 μm spacing) were collected at 14 min intervals. All cells express the membrane-targeted red fluorescent protein mTomato, except for rare recombinant clones in the UB tips that switch to express the membrane-targeted green fluorescent protein mGFP. The yellow dotted line in A and B indicates the basal surface of the UB ampulla, and the white box highlights an mGFP-positive UB cell about to undergo mitosis. **B, B′** and **B″,** six successive stages of UB

cell delamination, division and reinsertion. **B,** red/green merge; **B′,** mGFP channel only, **B″** 3D rendering of mGFP channel (the 3D rendering shows additional labeled cells not visible in the optical sections of B and B′. At 0′, the pre-mitotic cell has elongated into the lumen, but retains extensive contact with the basal surface (asterisk); at 14′, the cell has rounded and retains only a thin membranous process connecting it to the basal surface (asterisk); at 28′, cytokinesis has begun (arrows) and only the lower cell has apparently inherited the basal process; at 42′ – 56′, the tethered cell (blue arrow) reinserts at the original position in the surface epithelium (asterisk); by 84′, the two daughter cells have reinserted into the epithelium at separate sites, but retain an apical connection. This movie terminated before the two daughter cells completed cytokinesis, but other examples (e.g., Figure 1, Figure S1) show that cytokinesis is typically complete within 1–3 hours of mitosis. A time-lapse sequence of the 3D rendered cell division in **B″** is shown in Movie S4, and a similar analysis of a second dividing UB tip cell is shown in Figure S1.

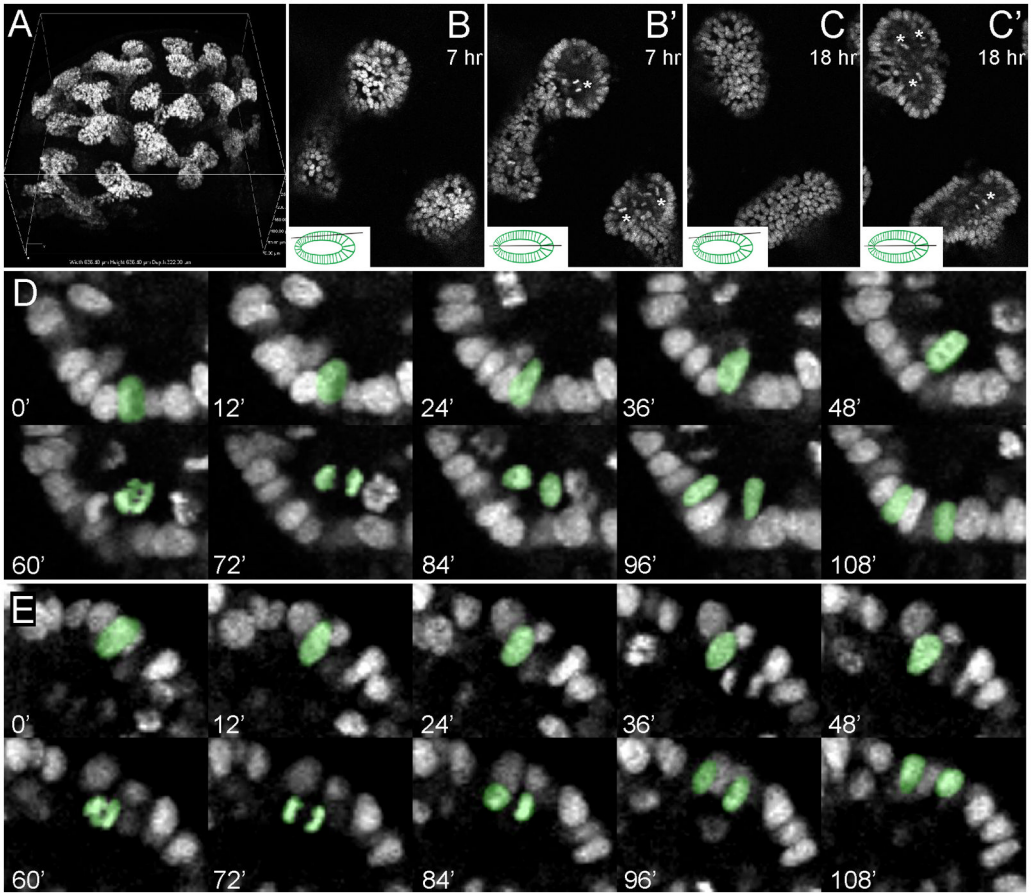

Figure 4. 4D analysis of mitoses during ureteric bud branching, using a nuclear fluorescent label

A, 3D rendering of an E12.5 *TcfLEF-H2BGFP* transgenic kidney, from a confocal image stack. Note the expression of H2BGFP only in the ureteric bud cells, and not in the surrounding mesenchymal cells. **B, B′, C, C′**, optical sections from an 18 hour culture of an E12.5 *TcfLEF-H2BGFP* transgenic kidney. B and C are optical sections at the level of the surface epithelium, while B′ and C′ are optical sections at a deeper level that bisects the UB lumen and the lateral edges of the epithelium (see inset diagrams). Asterisks in B′ and C′ indicate mitotic figures visible only at the level of the lumen. Complete 18 hr time-lapse movies, at the z-levels shown in B and C, are provided in Movie S6. A 3D image sequence showing the overall branching of the UB is provided in Movie S5. **D–G,** sequences of optical sections (at 12 minute intervals) in which mitotic events are visible. The pseudocolored nuclei in D and E first move in a luminal direction (0′ – 48′), then divide (60′ – 72′), then the daughter nuclei then reinsert in the surface epithelium at separate positions (84 – 108 min). The image sequences in D and E are also provided as Movie S7. See also Figure S2.

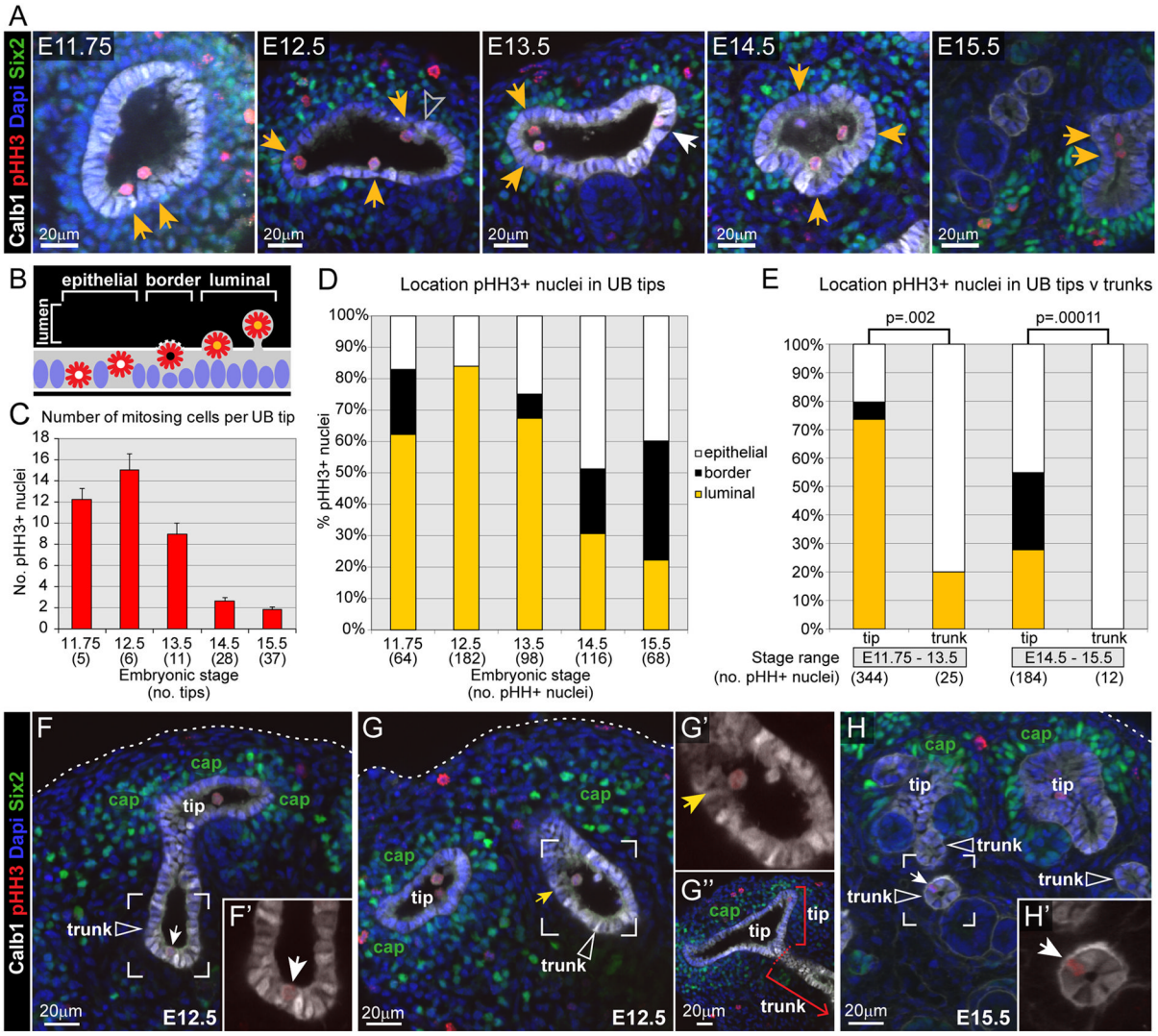

Figure 5. 3D confocal microscopic analysis of mitotic cells in ureteric tips vs. trunks *in vivo*

Whole mouse kidneys at stages from E11.75 to E15.5 were stained with markers for ureteric bud epithelium (anti-Calbindin1, white), mitotic cells (anti-pHH3, red), cap mesenchyme cells (anti-GFP to detect Six2GFP, green) and all nuclei (DAPI, blue), and the outer portion of each kidney (containing mostly tips and portions of the adjacent trunks) was examined by confocal microscopy. **A–D**, locations of mitotic cells in UB tips. **A,** representative optical sections through a ureteric tip at the indicated stages. Yellow arrows indicate pHH3+ cells located within the lumen (as diagrammed in **B**), and the white arrow indicates a pHH3+ cell within the epithelium at E13.5. See Figure S3 for examples of each type of pHH3+ cell diagrammed in B. Grey arrowhead in E12.5 indicates a Calbindin1+, pHH3- cell within the lumen. **C**, number of pHH3+ cells per ureteric tip (error bars indicate standard error of the mean). **D**, percentage of pHH3+ tip cells located within the lumen (yellow bars), at the lumen-epithelial border (black bars), or within the epithelium (white bars). **E**, comparison of pHH3+ cell locations in UB tips vs. trunks. Because of the rarity of mitotic cells in UB trunks, for this comparison the data were pooled into two groups: early (E11.75–E13.5) or later (E14.5–E15.5) stages. No pHH3+ cells were identified at the lumen-epithelial border in trunks. A Fisher's exact test of independence showed statistically significant differences in the distribution of pHH3+ nuclei between tip and trunk across the three locations (lumen –

yellow bars, lumen-epithelial border – black bars and epithelium – white bars), at both stage ranges (p values are shown). **F–H**, Examples of mitotic cells in UB trunks (indicated by open white arrowheads), which were distinguished from tips using 3D structural morphology and by the absence of adjacent Six2+ cap mesenchyme (labeled “cap” in green). The outer edge of the kidney is indicated by dotted white lines. **F** and **G**, E12.5 kidneys. **F and F′** show an epithelial pHH3+ trunk cell (white arrows), and **G** and **G′** a luminal pHH3+ trunk cell (yellow arrows). **G″** shows the terminal end of the trunk highlighted in G and G′, but in a different optical section where the dotted red line indicates the boundary between “tip” and “trunk”. **H** and **H′** show an example of a pHH3+ cell within the trunk epithelium at E15.5. 3–4 kidneys samples were examined at each stage. See also Figures S3 and S4 (for rendering and cell counting methods, and measurement of ureteric tip lumen volumes).

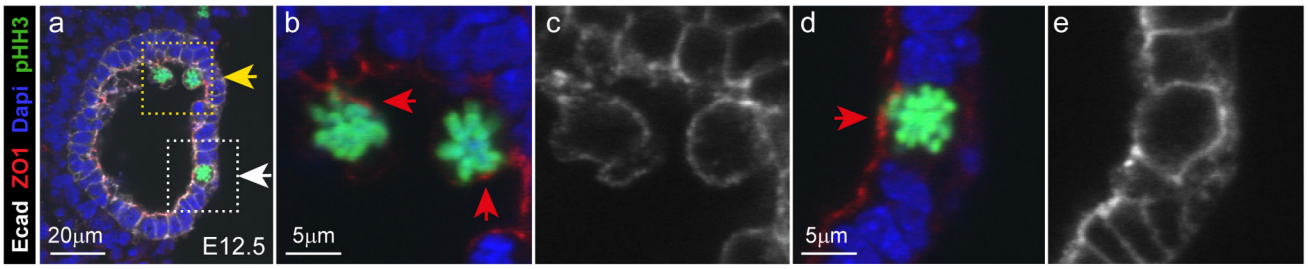

Figure 6. Mitotic cells in the ureteric tip lumen retain E-cadherin and ZO-1 expression

A, optical section of E12.5 mouse kidney fluorescently labeled with antibodies for E-cadherin (white), ZO-1 (red), pHH3 (green) and cell nuclei (DAPI, blue). Two of the pHH3+ cells are located in the lumen (yellow arrow) and one is within the epithelium (white arrow). B and C, enlargements of the yellow boxed area in A, showing that ZO-1 expression is localized to a specific subdomain (red arrows in **b**) on the E-cadherin labeled surface (**C**) of the two luminal pHH3+ tip cells. D and E, enlargement of the epithelial mitotic tip cell (white boxed area in a) shows that it expresses ZO-1 on its apical surface, in the same pattern as the non-mitotic (pHH3-) tip cells adjacent to it within the epithelium. See also Figure S5, and Figure S6, which shows additional examples.

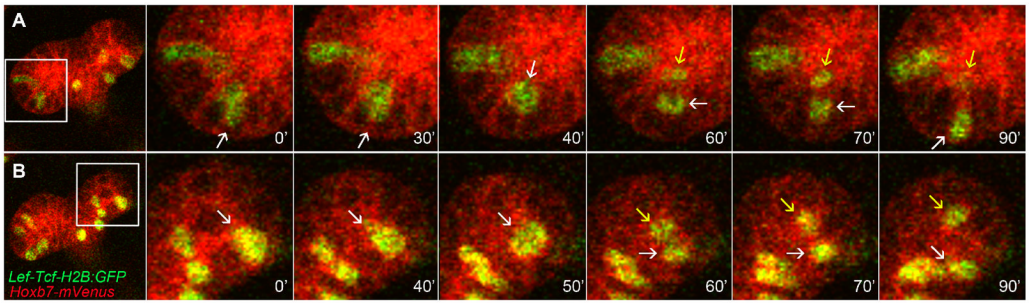

Figure 7. Mitotic cell dispersion occurs in E17.5 ureteric tips

An E17.5 kidney expressing the membrane marker Hoxb7/myr-Venus in all UB cells, and with mosaic expression of LEF/Tcf:H2B-GFP in a few UB tip cells, was cultured and imaged by confocal microscopy. The myr-Venus and H2B-GFP signals were separated by spectral imaging and linear unmixing, and myr-Venus was pseudo-colored red. The cell indicated by an arrow at 0 minutes (0′) divides at 60′, its daughters immediately separate (arrows), and they remain 1–2 cells distant at 90′(arrows).